



Research article

Preliminary evidence that bilateral scaphoid symmetry is not affected by hand dominance or biological sex: volumetric and geometric analysis using high-resolution computed tomography with 0.5 mm slice-thickness

Michael Roberts^{a,b}, Susie Lee^{a,b} , Amy Allen^{a,b,*}, Eliza Whiteside^{b,c,d}, Edward Bliss^{c,d}, Rose Nicol^{b,e}, Polly Burey^b, Tristan Shelley^b, Christopher Wall^a, Vivek Shridhar^a

^a Department of Orthopaedics, Toowoomba Hospital, Toowoomba QLD 4350, Australia

^b Centre for Future Materials, SIMPLE Hub, University of Southern Queensland, Toowoomba QLD 4350, Australia

^c School of Health and Medical Sciences, University of Southern Queensland, Toowoomba QLD 4350, Australia

^d Centre for Health Research, University of Southern Queensland, Toowoomba QLD 4350, Australia

^e Emergency Department, Toowoomba Hospital, Toowoomba QLD 4350, Australia



ARTICLE INFO

Keywords:

Scaphoid

Non union

Symmetry

Computed Tomography

ABSTRACT

The scaphoid bone has a unique anatomy that can lead to complicated injury healing including non-union with or without avascular necrosis and subsequent complex operative treatment. The use of imaging of contralateral bones for operative planning and implant creation such as bone grafting relies on the innate symmetry of the human body. Previous studies of scaphoid anatomy have demonstrated symmetry in three-dimensional space and volume in right-hand dominant individuals. There is a gap in the literature reporting on scaphoid symmetry in left-hand dominant individuals. This study used the computed tomography (CT) scans of 30 healthy participants to create three dimensional (3D) models of left and right scaphoids to assess their symmetry. These bilateral models were quantified with respect to volume, surface area, length, and iterative-closest point (ICP). Paired-sample t-tests found differences in the volumes of contralateral scaphoids in males however surface area, length, and ICP of the scaphoids was observed to be not significantly different suggesting symmetry using these measures. In females, there was a significant difference in length but not the other measures. These results support further investigation using larger sample sizes and greater representation of left hand dominant participants into the use of contralateral scaphoid CT scans in pre-operative planning for the manufacture of patient-specific implants.

1. Introduction

The scaphoid bone is named for the Greek “skaphe” or ‘boat’ [1]. The complex shape is concave in both ulnar and palmar axes and the long axis lies in an oblique plane [2,3]. The scaphoid is covered by approximately 75 % articular cartilage and it intersects with five bones; radius, lunate, trapezoid, trapezium, and capitate [4]. The blood supply of the scaphoid is by two branches of the radial artery, the superficial palmar and the dorsal scaphoid arteries. The scaphoid is vulnerable to vascular injury because the proximal pole is supplied solely by the retrograde intraosseous flow of the dorsal branch, as shown in Fig. 1 [5,6].

Scaphoid fractures are a common injury, accounting for 2–7 % of all fractures and 60 % of carpal bone fractures [7,8]. Fractures typically

occur in younger, active males [9]. Operative management is recommended for all displaced scaphoid fractures and considered for non-displaced fractures in younger, active patients with an aim of earlier return to work [10]. Delay to diagnosis and fracture displacement management are key risk factors in the development of non-union from poor fracture site immobilisation and subsequent proximal fragment necrosis [11]. Management of scaphoid non-union aims to restore anatomical alignment with fixation methods including: volar plates, or headless compression screws with or without the use of vascular and non-vascularised grafts during fixation [12–14]. Planning for these surgeries can involve using contralateral imaging to inform reduction and guide fixation as well as for estimating the amount of graft bone required [15].

* Corresponding author at: Centre for Future Materials, University of Southern Queensland, West Street, Toowoomba, Australia 4350.

E-mail addresses: Amy.allen@unisq.edu.au, Amy.allen@health.qld.gov.au (A. Allen).

<https://doi.org/10.1016/j.ejrad.2025.112073>

Received 21 November 2024; Received in revised form 6 March 2025; Accepted 26 March 2025

Available online 10 April 2025

0720-048X/© 2025 The Author(s). Published by Elsevier B.V. This is an open access article under the CC BY-NC license (<http://creativecommons.org/licenses/by-nc/4.0/>).

Recent anatomical studies have utilised commercial imaging software to process Digital Imaging and Communications in Medicine (DICOM) files into three dimensional (3D) geometric objects. These DICOM files are produced from CT or magnetic resonance imaging (MRI) scans and have been demonstrated in cadaveric studies to be accurate to within 0.63 mm of the original bone [16,17]. This error is acceptable in clinical practice when using CT as this modality does not account for cartilage thickness, which has been shown to be approximately 0.84 mm [18]. Differences in bone morphology and geometry can be analysed using a mesh resolution to create point-to-point references. The sequential alignment of these reference points between two objects is referred to as the iterative closest point (ICP) and can be used as a measure of surface variation between objects. These measurements can then be used to analyse the geometric variability between bones, including their landmarks [19,20]. Given the ICP can be used in this way, differences in ICP will detect differences in previously described parameters of scaphoid symmetry such as tubercle height, waist circumference, and width of the main sulcus [21].

Symmetry has previously been demonstrated in the scaphoid using CT with slice thickness of 0.62 mm or thicker [21–24] but has not been investigated in CT with a slice thickness of 0.5 mm. Ten Berg et al. assessed the symmetry of scaphoids from 19 healthy adults in a 3D space, measuring translation and rotation from a central axis drawn between the proximal and distal poles using a CT slice thickness of 0.67 mm [22]. The results showed no significant difference between the sides when comparing translation and rotation of distal poles. Letta et al. analysed 3D scaphoid models derived from CT scans with an axial resolution of 1.0 mm and processed to observe surface-to-surface deviation in 26 healthy adults. The measurements in this study included volume, surface area, and length. No significant difference in sides were observed within these parameters however significant difference was observed in surface-to-surface variation in circumference of the waist, base, and height of the tubercle and width of the main sulcus [21]. There are no more recent studies that have further evaluated symmetry of the scaphoid using higher density CT scans, however researchers have analysed symmetry elsewhere in the body, in particular the foot and

ankle [17,25–27], the femur [28,29] and the bones of the face and jaw [30–33]. These studies have shown variable symmetry throughout the skeleton. For example, asymmetry is prominent in the facial bones and jaw [31–33] with only one study demonstrating symmetry [30]. In the case of the femur, however, research by Sparks et al. [28] and Zhang et al. [29] confirmed symmetry using high resolution CT and suggested that CT of contralateral femurs can be reliably used for surgical planning. There is variability in the results from previous analyses of the foot and ankle with some studies demonstrating symmetry and others not. Vuurberg et al. [26] demonstrated tibia asymmetry however acknowledges that this requires further investigation as to whether the differences observed are clinically significant. In the upper extremities, symmetry has more recently been studied in the lunate and radius. These studies have demonstrated that these bones are not symmetrical with high resolution CT however the differences between them may not be clinically significant [20,27].

Surgical management of scaphoid fracture aims to achieve fracture union and restore functional movement. Scaphoid non-union creates greater difficulty in this process by the development of carpal instability, humpback deformity, and Scaphoid Non-union Advanced Collapse (SNAC) arthritic changes [34]. The accuracy of the surgical management of scaphoid non-union varies with methodologies used. Traditional scaphoid fixation relies on intra-operative imaging to correctly restore the scaphoid length and angulation [35]. More recent surgical approaches include robotic assistance, intra-operative CT guidance, and surgical guides modelled on uninjured contralateral scaphoids. The results of these approaches have demonstrated improved radiological outcomes and equivalent clinical outcomes across all measures [14,35]. The degree to which the radiological outcome affects long term outcomes for patients is not conclusive and requires further investigation [14].

The aim of the current pilot study was to investigate the symmetry of bilateral scaphoids in 30 healthy adults by measuring outcomes of volume and geometric variation using high-resolution CT scans (0.5 mm slice thickness). Previous studies have used lower resolution CT scans [21,22]. The secondary aims were to determine the effect of biological

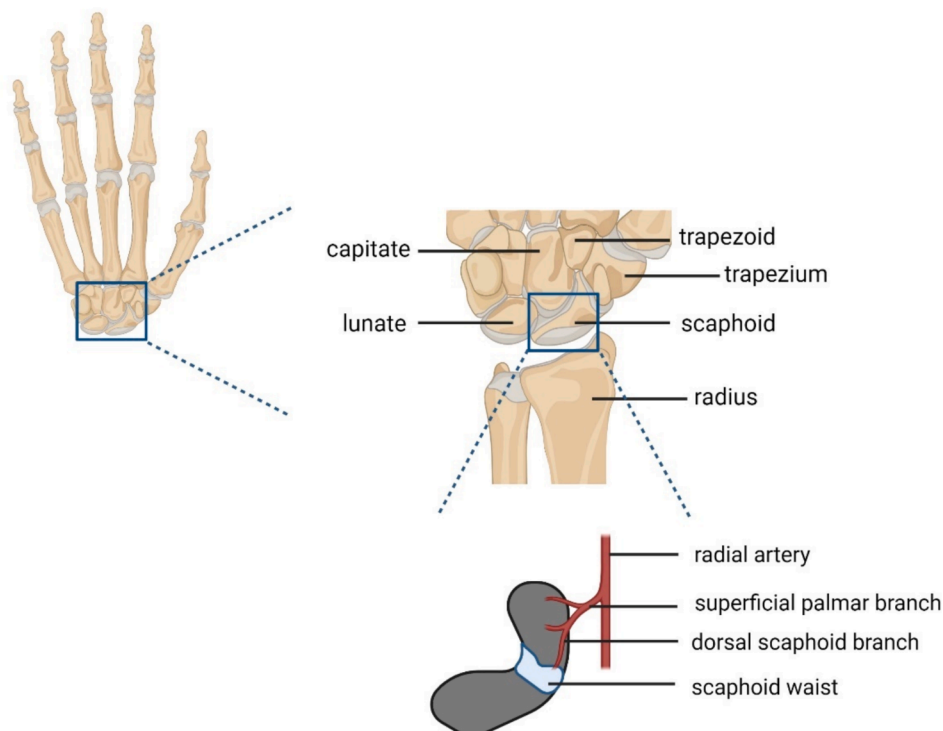


Fig. 1. Relational anatomy and vascular supply of the scaphoid bone.

sex and hand dominance on scaphoid symmetry. The effect of biological sex on scaphoid symmetry has not been previously described. There is limited current evidence evaluating the effect of hand dominance on scaphoid symmetry, in particular on the symmetry of scaphoids of left-handed individuals [21,22,36]. Our study aims to address these gaps in current knowledge about scaphoid symmetry to provide further evidence for the usefulness of contralateral high resolution CT measurements for pre-operative surgical planning.

2. Materials and methods

2.1. Data acquisition

Ethics approval was granted by the Darling Downs Health Human Research and Ethics Committee and informed consent was obtained prior to participation. Thirty healthy volunteers participated in this study (17 males and 13 females; 24 right-handed and 6 left-handed; average age: 35 years; range 24–60 years; standard deviation 11.6 years). The participants had no history of wrist injury or other musculoskeletal disorders.

A high-resolution CT scan (Canon Aquilion ONE, Otawara, Japan) of both wrists was obtained using a standardised method to immobilise the wrists 2 cm apart, with a slice thickness of 0.5 mm. The voltage was 80kVp, field of view set to 80.2 and rotation time 0.25 sec. The raw DICOM files were used for measurements and subsequent 3D image analysis.

2.2. Assessment of volume

DICOM files were processed using Vitrea Advanced Visualization (Canon Medical Systems, Otawara, Japan). Manual isolation of the scaphoid was performed using the bone segment function with removal of surrounding carpal bones. The remove fragment function was used to automate removal of remaining smaller fragments separate to the scaphoid bone. The Vitrea volume function was used to measure volume in millimetres cubed (mm³). The stereolithography (STL) file created for each scaphoid was used for further assessment.

2.3. Assessment of geometry

STL files were imported into MeshLab 2022 (CNR-ISTI, Rome, Italy). Scaphoids were imported and encased in polygonal mesh which was processed with quadratic edge collapse decimation with the quality threshold set to 1 and boundary preserving weight of 1. The model was cleaned by removing duplicate vertices and faces with automated functions in MeshLab. The “Compute geometric measures” function was used to automate calculation of the scaphoid surface areas. Right scaphoids were imported first. Left scaphoids were then imported and had faces inverted using the “Invert faces orientation” function. The left scaphoid was coarsely aligned with the contralateral bone using the align function, using four manually selected points on the scaphoid. These were the tubercle, apex of the proximal pole, apex of the capitate ridge, and apex of the dorsal ridge. Alignment of the pair of scaphoids was refined and automated with the ICP function in MeshLab, which was also used to calculate the ICP.

2.4. Statistical analysis

Statistical analysis of the data was conducted using Statistical Package for the Social Sciences (SPSS, IBM, Chicago, USA). The Kolmogorov-Smirnov and Shapiro-Wilk tests were applied to the age of participants, which demonstrated that participants were not normally distributed with regards to age ($p < 0.001$). Skewness was 0.98 and kurtosis was -0.57 . Descriptive statistics and the Kolmogorov-Smirnov test for normality demonstrated normality and equal variance across all dependent variables. Paired-sample t-tests were used to investigate

differences in the means for volume, surface area, and length between left and right scaphoids. The ICP was used to detect variability between contralateral scaphoid surface geometry. Contralateral differences were measured by subtracting left hand measurements from the right hand measurements across all measures and obtaining absolute values of these differences.

3. Results

There were no significant differences in volume, surface area, length, or ICP between right hand dominant, and left hand dominant individuals (two sample t-tests $p > 0.05$), as summarised in Table 1.

As is shown in Table 2, the mean volume, surface area and length of left scaphoids was significantly larger in left hand dominant males compared with right hand dominant males. This was not reciprocated in right hand dominant males. The small sample size of two left hand dominant males is a major limitation here, where an outlier with a larger scaphoid may have skewed these results.

There was no statistical difference between parameters in right and left handed females as shown in Table 3.

Comparisons between male and female scaphoids demonstrated significantly greater volume, surface area, and length in males (two-sample t-test $p < 0.01$). Male scaphoid dimensions were greater than female counterparts as shown in Table 4. There was no significant difference in the ICP between the two groups (two-sample t-test $p = 0.40$).

Across the sampled population there was a significant difference between the volume of right and left scaphoids. The mean difference between these volumes was 165.63 mm³ (standard deviation 115.00 mm³). There was no significant difference between the surface area or length of left and right scaphoids. This is shown in Table 5.

As shown in Table 6, the differences between the volume of left and

Table 1
Summary and analysis of measurements by hand dominance.

	Right hand dominant (n = 24)	Left hand dominant (n = 6)	Both Groups (n = 30)	Significance between groups (two-tailed p < 0.05)
Mean Volume	2879 ± 832	2658 ± 1223	2767 ± 866	0.60
Right +/- standard deviation (mm ³)				
Mean Volume Left +/- standard deviation (mm ³)	2718 ± 809	2728 ± 1222	2720 ± 881	0.98
Mean Surface Area Right +/- standard deviation (mm ²)	1198 ± 256	1106 ± 348	1179 ± 273	0.47
Mean Surface Area Left +/- standard deviation (mm ²)	1173 ± 214	1122 ± 339	1163 ± 238	0.65
Mean Length Right +/- standard deviation (mm)	26.09 ± 3.29	25.65 ± 3.73	26.00 ± 3.32	0.79
Mean Length Left +/- standard deviation (mm)	26.39 ± 2.62	25.90 ± 3.49	26.29 ± 2.75	0.79
Mean iterative closest point (ICP) +/- standard deviation (mm)	0.25 ± 0.00	0.27 ± 0.07	0.26 ± 0.07	0.45

Table 2
Summary and analysis of measurements by hand dominance in males.

	Right hand dominant (n = 15)	Left hand dominant (n = 2)	Both Groups (n = 17)	Significance between groups (two-tailed p < 0.05)
Mean Volume	3380 ±	4100±	3464.71	0.13
Right +/- standard deviation (mm ³)	587.42	777.82	± 630.01	
Mean Volume	3205.33	4170 ±	3318.82	0.047
Left +/- standard deviation (mm ³)	±579.59	749.53	± 657.03	
Mean Surface Area	1354.11 ±	1513.20 ±	1372.82	0.21
Right +/- standard deviation (mm ²)	164.20	158.24	± 167.18	
Mean Surface Area	1314 ±	1517.33 ±	1337 ±	0.049
Left +/- standard deviation (mm ²)	121.02	184.07	139.62	
Mean Length	27.93 ± 2.15	30.16 ±	28.19 ±	0.18
Right +/- standard deviation (mm)		0.66	2.15	
Mean Length	27.71 ± 1.74	30.51 ±	28.04 ±	0.043
Left +/- standard deviation (mm)		0.14	1.88	
Mean iterative closest point (ICP) +/- standard deviation (mm)	0.27 ± 0.06	0.25 ± 0.04	0.26 ± 0.06	0.76

right scaphoids in individual males was statistically significant with a magnitude of 125.31 mm³ (standard deviation 98.10 mm³). The surface area and lengths within an individual male did not significantly differ. This is consistent with the results from the total population of scaphoids examined in this study.

The differences between the length of left and right scaphoids in individual females was statistically significant with a magnitude of 1.05 mm (standard deviation 1.06 mm). The volume and lengths within an individual female did not significantly differ. This is demonstrated in Table 7. The mean differences observed for each parameter did not differ between male and female groups (p > 0.05 for all parameters).

As is shown in Table 8, in right hand dominant individuals, the right scaphoid was significantly larger in volume than the left. The magnitude of this difference was 185.38 mm³ (standard deviation 116.30 mm³). There were no significant differences in length or surface area. This is consistent with the results from the total population of scaphoids examined in this study and with the results of the male population.

In left handed individuals, there was no statistically significant difference between any of the parameters assessed. This is shown in Table 9. The mean differences observed for each parameter did not differ between right and left hand dominant groups (p > 0.05 for all parameters).

In males, the average difference between right and left scaphoid volumes was 196.47 mm³, between surface areas 74.91 mm² and between lengths 1.74 mm. In females, the average difference between right and left scaphoid volumes was 125.31 mm³, between surface areas 42.41 mm² and between lengths 1.06 mm. None of these differences were significantly different between males and females (independent sample t-test p > 0.05).

Table 3
Summary and analysis of measurements by hand dominance in females.

	Right hand dominant (n = 9)	Left hand dominant (n = 4)	Both Groups (n = 13)	Significance between groups (two-tailed p < 0.05)
Mean Volume	2043.22 ±	1937.50 ±	2010.69	0.66
Right +/- standard deviation (mm ³)	363.62	460.03	± 378.99	
Mean Volume	1904.44 ±	2007.50 ±	1936.15	0.65
Left +/- standard deviation (mm ³)	323.31	471.05	± 357.22	
Mean Surface Area	936.49 ±	901.81 ±	925.82 ±	0.70
Right +/- standard deviation (mm ²)	137.71	164.90	140.42	
Mean Surface Area	938.60 ±	924.75 ±	932.34 ±	0.83
Left +/- standard deviation (mm ²)	84.20	157.13	104.61	
Mean Length	23.01 ±	23.39 ±	23.12 ±	0.78
Right +/- standard deviation (mm)	2.44	1.64	2.16	
Mean Length	24.07 ±	23.86 ±	24.01 ±	0.86
Left +/- standard deviation (mm)	2.03	1.87	1.90	
Mean iterative closest point (ICP) +/- standard deviation (mm)	0.22 ± 0.08	0.29 ± 0.08	0.24 ± 0.08	0.22

There was no significant difference between the differences of the means of male and female groups across volume (p = 0.09), surface area (p = 0.06), or length (p = 0.19) measurements.

Fig. 2 plots the ICP between left and right scaphoids in the four groups examined. It shows that there is no statistically significant differences in the ICP between groups. The maximum ICP in the population examined was 0.42 mm. The mean ICP across the sampled group was 0.26 mm.

Fig. 3 demonstrates the greatest area of surface variation between the scaphoid pair measured as ICP.

4. Discussion

The aim of this pilot study was to investigate the symmetry of bilateral scaphoids in healthy adults by measuring outcomes of volume, length, surface area and geometric variation using high-resolution CT scans (0.5 mm slice thickness). The secondary aims were to determine the effect of biological sex and hand dominance on scaphoid symmetry.

Our results have suggested that scaphoids in healthy adults are largely symmetrical. They differed statistically in their volume in our overall group, as well as in the male population and in right handed individuals. In females, they statistically differed in their length, but not in volume or surface areas. Though there were statistically significant differences in these parameters, the clinical significance of this is not known. The volume of bone defects in scaphoid fractures has not been well examined, therefore the implications of this difference of 165 mm³ on the management of scaphoid fracture non-union are unknown. 165 mm³, is less than 6 % of the volume of the average scaphoid observed in our study. When considering the practical implications of this difference

Table 4
Summary of 3D scaphoid measurements by biological sex.

	Females (n = 13)	Males (n = 17)	Relative size of male to female (%)	Significance (two-tailed p)
Mean Volume Right scaphoid +/- standard deviation (mm ³)	2010 ± 379	3346 ± 654	139.9	<0.01
Mean Volume Left scaphoid +/- standard deviation (mm ³)	1936 ± 257	3319 ± 657	141.7	<0.01
Mean Surface Area Right scaphoid +/- standard deviation (mm ²)	926 ± 140	1373 ± 167	132.6	<0.01
Mean Surface Area Left scaphoid +/- standard deviation (mm ²)	934 ± 105	1338 ± 140	130.2	<0.01
Mean Length Right scaphoid +/- standard deviation (mm)	23.13 ± 2.16	28.19 ± 2.15	117.9	<0.01
Mean Length Left scaphoid +/- standard deviation (mm)	24.00 ± 1.90	28.04 ± 1.87	114.4	<0.01
Mean iterative closest point (ICP) +/- standard deviation (mm)	0.24 ± 0.08	0.26 ± 0.06	108.3	0.40

Table 5
Summary of 3D scaphoid measurements, comparing left and right sides.

	Right scaphoid (n = 30)	Left scaphoid (n = 30)	Significance between sides (2-tailed, paired T test, p < 0.05)
Mean volume ± standard deviation (mm ³)	2834.63 ± 903.03	2719.67 ± 887.85	p = 0.0007
Mean surface area ± standard deviation (mm ²)	1182.46 ± 269.96	1159.70 ± 240.79	p = 0.102
Mean length ± standard deviation (mm)	26.05 ± 3.27	26.30 ± 2.82	p = 0.401

Table 6
Summary of 3D scaphoid measurements in males, comparing left and right sides.

	Right scaphoid (n = 17)	Left scaphoid (n = 17)	Significance between sides (2-tailed, paired T test, p < 0.05)
Mean volume ± standard deviation (mm ³)	3464.71 ± 630.01	3318.82 ± 657.03	p = 0.004
Mean surface area ± standard deviation (mm ²)	1372.82 ± 167.18	1337.92 ± 139.62	p = 0.11
Mean length ± standard deviation (mm)	28.19 ± 2.15	28.04 ± 1.88	p = 0.80

in clinical practice when surgically reconstructing a scaphoid non-union with bone loss, this small volume may be within the range of expected human error in volume restoration. The ICP analysis revealed that the surface anatomy of scaphoids was symmetrical. The average difference in surface anatomy was 0.255 mm and the maximum difference was

Table 7
Summary of 3D scaphoid measurements in females, comparing left and right sides.

	Right scaphoid (n = 13)	Left scaphoid (n = 13)	Significance between sides (2-tailed, paired T test, p < 0.05)
Mean volume ± standard deviation (mm ³)	2010.69 ± 378.99	1936.15 ± 357.22	p = 0.09
Mean surface area ± standard deviation (mm ²)	925.82 ± 140.42	934.34 ± 104.61	p = 0.57
Mean length ± standard deviation (mm)	23.13 ± 2.16	24.01 ± 1.90	p = 0.02

Table 8
Summary of 3D scaphoid measurements in right hand dominant individuals, comparing left and right sides.

	Right scaphoid (n = 24)	Left scaphoid (n = 24)	Significance between sides (2-tailed, paired T test, p < 0.05)
Mean volume ± standard deviation (mm ³)	2878.71 ± 832.50	2717.50 ± 809.14	p = 0.00002
Mean surface area ± standard deviation (mm ²)	1197.50 ± 256.24	1173.22 ± 214.12	p = 0.16
Mean length ± standard deviation (mm)	26.09 ± 3.29	26.39 ± 2.62	p = 0.28

Table 9
Summary of 3D scaphoid measurements in left hand dominant individuals, comparing left and right sides.

	Right scaphoid (n = 6)	Left scaphoid (n = 6)	Significance between sides (2-tailed, paired T test, p < 0.05)
Mean volume ± standard deviation (mm ³)	2658.33 ± 1222.71	2728.33 ± 1221.69	p = 0.11
Mean surface area ± standard deviation (mm ²)	1105.61 ± 347.85	1122.28 ± 339.45	p = 0.35
Mean length ± standard deviation (mm)	25.65 ± 3.73	25.90 ± 3.49	p = 0.44

0.402 mm. As previously discussed, this small difference is not clinically significant when the average scaphoid cartilage thickness is 0.84 mm [18], which can cause variability in the surface anatomy greater than what was observed in our study using CT scans. The ICP analysis supports the hypothesis of contralateral scaphoid symmetry.

The results of this study were consistent with the findings from previous research that has used lower resolution CT [21,22,24] and magnetic resonance imaging (MRI) [37] to report on scaphoid symmetry (restricted to right-hand dominant participants) with respect to total surface area. This study's findings support the utilisation of CT scans of uninjured contralateral scaphoids in pre-operative surgical planning for the correction of acute scaphoid fractures and non-union.

One of the secondary aims of this study was to evaluate the effect of hand dominance on scaphoid measurements. Right handed individuals had a significant difference in scaphoid volume. In left handed individuals there was no statistically significant difference in recorded parameters, however we acknowledge that the sample size of left handed individuals is small and may mask a significant result. Examining the magnitude of the differences in recorded volume, surface area,

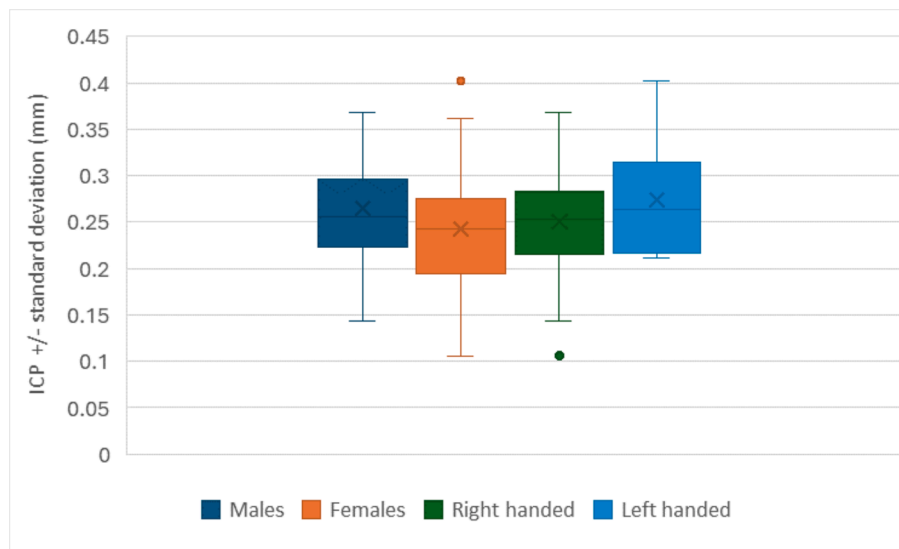


Fig. 2. Iterative closest point between right and left scaphoids.

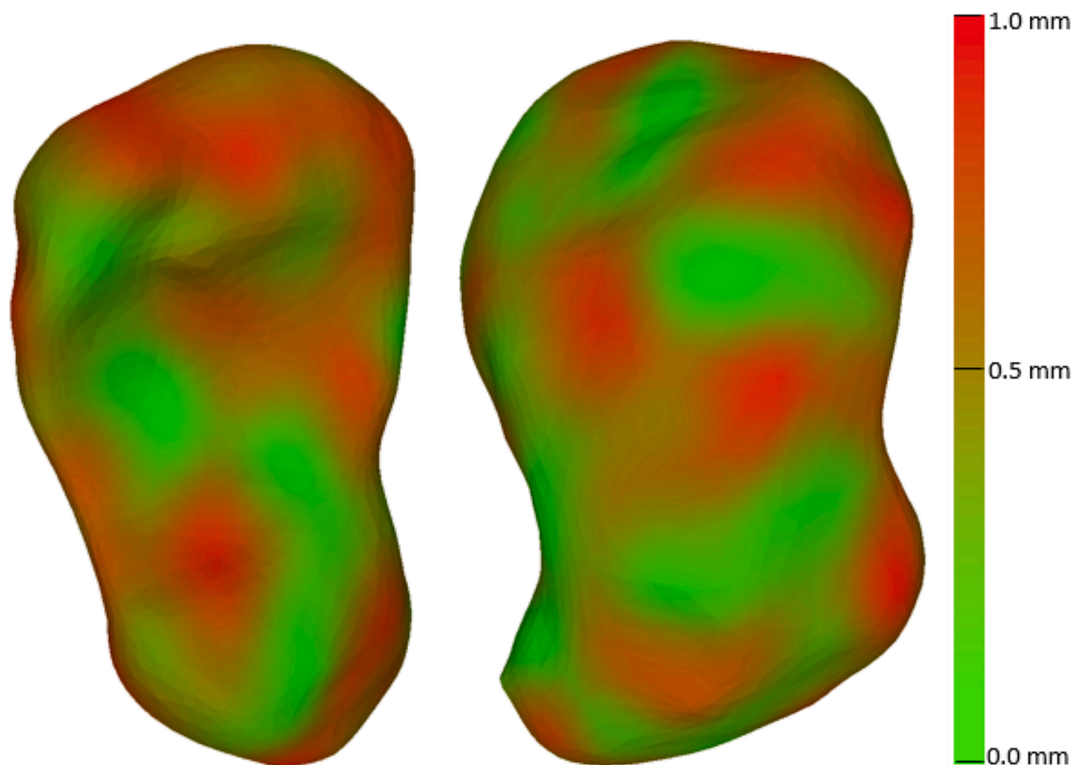


Fig. 3. Greatest scaphoid pair surface variation between contralateral sides measured as iterative closest point. The areas of maximal difference are highlighted in red and less difference in green.

and length in left handed individuals, they are all less than their counterparts in the right handed group. From our review of the literature, this is one of only a few studies to report on the effect of ‘handedness’ on scaphoid symmetry. Ten Berg et al confirmed scaphoid symmetry in right-handed individuals only as left-handed participants were not included [22]. Other studies have not included hand dominance in their analyses [21,24,36,37]. Smith et al. utilised MRI imaging to examine 30 healthy individuals without reporting handedness and Letta et al. utilised CT imaging to examine 26 healthy right-handed individuals [21,37]. The measurement of symmetry shared between the two studies was scaphoid length. Other studies have reported a right to left

difference of 0.00 ± 0.53 mm [37] and 0.2 ± 0.4 mm [21] respectively.

Further comparison of geometric measurements of symmetry have only been reported by Letta et al. with measurements of volume and surface deviation measured by ICP [21]. Volumetric measurements reported in this study are similar to Letta et al. with an average volume of 95.3 ± 66.2 compared to this study’s 115.0 ± 167.1 mm³ [21]. In particular, the results when reported by handedness did not significantly differ with the right-handed individuals recording larger right scaphoid volumes and left-handed individuals’ results demonstrating marginally larger left scaphoids.

The findings of this study may have implications for current and

future practice. New methods of scaphoid fixation have utilised advances in CT technology that enable a reduction in the size of isotropic voxels and slice thickness to a size appropriate for surgical planning of 0.4–0.6 mm [38]. This technique has been used in the development of surgical guides to aide correction of the humpback deformity developed as a sequelae of scaphoid non-union [39–42]. This technique has further been applied to the limited development of scaphoid implants used for the management of carpal conditions including scaphoid non-union and pan-carpal osteoarthritis [41,42]. This study improves confidence in the use of contralateral imaging in surgical planning for both right and left hand dominant patients. It demonstrates that CT imaging of the contralateral scaphoid can be used as a surface model for the pre-injury state of the injured side. An injured scaphoid that has progressed to non-union can have variable amounts of bone loss and deformity, making the task of planning for the reconstruction of these bones to their pre-injury state challenging [43]. In these cases, surgical planning may be able to be improved by using the un-injured scaphoid as a reference for pre-operative templating for reconstruction of the injured side [44].

A limitation of this study is that the use of CT images restricts the ability to image articular cartilage therefore the estimates would deviate from the true size of the scaphoid. A further limitation is the small sample size, reducing the power of statistical conclusion. We performed a post hoc power analysis that demonstrated a required sample population of 962. This was a pilot study and a sample of convenience was used. Future studies may be able to expand on our findings with an increased sample size to minimise type 2 error. However, in the setting of other results investigating bilateral symmetry, we would expect there to be no greater difference in left-handed individuals. Data collected from participants did not include racial or regional information which may have impacted results. This impact is not able to be assessed and is a limitation of our study.

In conclusion, using high-resolution 0.5 mm thickness CT scans demonstrated non-significant differences in symmetry in the geometry of bilateral scaphoids, across the biological sexes and handedness. There were statistically significant differences in scaphoid volume for males and length for females however the clinical significance of this difference in the application of contralateral CT imaging for surgical planning is not known. The shape of contralateral scaphoids was found to be symmetrical by ICP analysis. The findings of this study support further investigation into the use of contralateral scaphoid imaging using high-resolution 0.5 mm thickness CT in planning scaphoid non-union operative correction.

Ethical approval

Darling Downs Health Human Research Ethics Committee.

CRedit authorship contribution statement

Michael Roberts: Writing – original draft, Software, Formal analysis, Data curation, Conceptualization. **Susie Lee:** Writing – review & editing, Methodology, Formal analysis. **Amy Allen:** Formal analysis, Writing – review & editing. **Eliza Whiteside:** Formal analysis, Funding acquisition, Methodology, Project administration, Supervision, Writing – original draft, Writing – review & editing. **Edward Bliss:** Formal analysis, Writing – review & editing. **Rose Nicol:** Writing – original draft. **Polly Burey:** Funding acquisition, Writing – original draft, Writing – review & editing. **Tristan Shelley:** Funding acquisition, Writing – review & editing. **Christopher Wall:** Conceptualization, Formal analysis, Methodology, Supervision, Writing – original draft, Writing – review & editing. **Vivek Shridhar:** Conceptualization, Formal analysis, Investigation, Methodology, Supervision, Writing – original draft, Writing – review & editing.

Informed consent

Provided by all participants.

Funding

This research has been funded by the Australian Department of Education through a Regional Research Collaboration (RRC) grant. This funding has allowed the establishment of the University of Southern Queensland-led SIMPLE Hub where this research has been conducted. The project was also funded by a Toowoomba Hospital Foundation Pure Land Learning College Research Grant.

Declaration of competing interest

The authors declare that they have no known competing financial interests or personal relationships that could have appeared to influence the work reported in this paper.

Acknowledgements

Sustainable Industry Manufacturing for Long-Term Ecosystems (SIMPLE) Hub Regional Research Collaboration (RRC) grant, Department of Education, Australian Government, and Toowoomba Hospital Foundation Pure Land Learning College Research Grant.

References

- [1] M. Amin, M. Abdelaal, Operative Treat. Scaphoid Nonunion. 89 (2021) 2023–2033, <https://doi.org/10.21608/mjcu.2021.203337>.
- [2] R. Sendher, A.L. Ladd, The scaphoid, *Orthop. Clin. North Am.* 44 (1) (2013) 107–120.
- [3] J. Eschweiler, et al., Anatomy, biomechanics, and loads of the wrist joint, *Life (Basel)* 12 (2) (2022).
- [4] L.E. Wessel, S.W. Wolfe, Scapholunate instability: diagnosis and management - anatomy, kinematics, and clinical assessment - part I, *J. Hand Surg. Am.* 48 (11) (2023) 1139–1149.
- [5] L.M. Hove, Epidemiology of scaphoid fractures in Bergen, Norway, *Scand. J. Plast. Reconstr. Surg. Hand Surg.* 33 (4) (1999) 423–426.
- [6] M. Le Mapihan, et al., Arthroscopic preservation of the scaphoid's blood supply during nonunion treatment, *J Hand Surg Eur* 47 (4) (2022) 420–422.
- [7] G. Testa, et al., Comparison between vascular and non-vascular bone grafting in scaphoid nonunion: a systematic review, *J. Clin. Med.* 11 (12) (2022).
- [8] M. Clementson, A. Björkman, N.O.B. Thomsen, Acute scaphoid fractures: guidelines for diagnosis and treatment, *EFORT Open Rev* 5 (2) (2020) 96–103.
- [9] P. Jörgsholm, et al., Epidemiology of scaphoid fractures and non-unions: a systematic review, *Handchir. Mikrochir. Plast. Chir.* 52 (5) (2020) 374–381.
- [10] P. Prabhakar, et al., Factors associated with scaphoid nonunion following early open reduction and internal fixation, *J Wrist Surg* 9 (2) (2020) 141–149.
- [11] E.D. Patterson, et al., Risk factors for the development of persistent scaphoid non-union after surgery for an established non-union, *Hand (N Y)* (2024) 15589447231219523.
- [12] N. Nagura, et al., Correction of humpback and DISI deformities by vascularized bone grafting in patients with scaphoid nonunion, *Sicot j* 7 (2021) 13.
- [13] J.P. Higgins, A.M. Giladi, Scaphoid nonunion vascularized bone grafting in 2021: is avascular necrosis the sole determinant? *J. Hand Surg. Am.* 46 (9) (2021) 801–806. e2.
- [14] L.X. Li, A.E. Kedgley, M.D. Horwitz, A review of the use of 3D printing technology in treatment of scaphoid fractures, *J. Hand Surg. Asian Pac.* 28 (1) (2023) 22–33.
- [15] L. Nagy, Kahnbeinseudarthrose: computerassistierte virtuelle Planung der Rekonstruktion, *Handchir. Mikrochir. Plast. Chir.* 52 (05) (2020) 435–440.
- [16] J.M. Stephen, et al., Comparative accuracy of lower limb bone geometry determined using MRI, CT, and direct bone 3D models, *J. Orthop. Res.* 39 (9) (2021) 1870–1876.
- [17] A.S. Gabrielli, et al., Bilateral symmetry, sex differences, and primary shape factors in ankle and Hindfoot bone morphology, *Foot Ankle Orthop.* 5 (1) (2020) 2473011420908796.
- [18] D.C. Moore, et al., μ CT-generated carpal cartilage surfaces: validation of a technique, *J. Biomech.* 44 (13) (2011) 2516–2519.
- [19] D. Gibelli, et al., Assessing symmetry of zygomatic bone through three-dimensional segmentation on computed tomography scan and “mirroring” procedure: a contribution for reconstructive maxillofacial surgery, *J. Craniomaxillofac. Surg.* 46 (4) (2018) 600–604.
- [20] E. Hong, D.S. Kwak, I.B. Kim, Morphological symmetry of the radius and ulna-contralateral forearm bones utilize as a reliable template for the opposite side? *PLoS One* 16 (10) (2021) e0258232.

- [21] C. Letta, A. Schweizer, P. Fürtstahl, Quantification of contralateral differences of the scaphoid: a comparison of bone geometry in three dimensions, *Anat. Res. Int.* 2014 (2014) 904275.
- [22] P.W. ten Berg, et al., Three-dimensional assessment of bilateral symmetry of the scaphoid: an anatomic study, *Biomed Res. Int.* 2015 (2015) 547250.
- [23] R.M. Patterson, et al., Carpal bone anatomy measured by computer analysis of three-dimensional reconstructions of computed tomography images, *J. Hand Surg. Am.* 20 (6) (1995) 923–929.
- [24] G. Schmidle, et al., Intraosseous rotation of the scaphoid: assessment by using a 3D CT model—an anatomic study, *Eur. Radiol.* 24 (6) (2014) 1357–1365.
- [25] J. Verbakel, et al., Symmetry of the left and right tibial plafond; a comparison of 75 distal tibia pairs, *Eur. J. Trauma Emerg. Surg.* 50 (6) (2024) 2877–2882.
- [26] G. Vuurberg, et al., Lower leg symmetry: a Q3D-CT analysis, *Surg. Radiol. Anat.* 44 (6) (2022) 851–860.
- [27] N. Tümer, et al., Three-dimensional analysis of shape variations and symmetry of the fibula, tibia, calcaneus and talus, *J. Anat.* 234 (1) (2019) 132–144.
- [28] C.A. Sparks, S.J. Decker, J.M. Ford, Three-dimensional morphological analysis of sex, age, and symmetry of proximal femurs from computed tomography: application to total hip arthroplasty, *Clin. Anat.* 33 (5) (2020) 731–738.
- [29] W. Zhang, et al., Optimizing femur symmetry judgment using three-dimensional data correction scheme in fractures of the proximal femur, *Injury* 53 (6) (2022) 2172–2179.
- [30] N. Morgan, et al., Three-dimensional quantification of skeletal midfacial complex symmetry, *Int. J. Comput. Assist. Radiol. Surg.* 18 (4) (2023) 611–619.
- [31] J. Zhao, et al., 3-dimensional analysis of hard- and soft-tissue symmetry in a Chinese population, *BMC Oral Health* 23 (1) (2023) 432.
- [32] I.O. Aiupova, et al., Lower jawbone structures symmetry evaluation using cone beam computed tomography, *Stomatologiia (Mosk)* 102 (6) (2023) 33–38.
- [33] P. Santander, et al., Comprehensive 3D analysis of condylar morphology in adults with different skeletal patterns - a cross-sectional study, *Head Face Med.* 16 (1) (2020) 33.
- [34] R. Samade, H.M. Awan, Surgical treatment of scaphoid fractures: recommendations for management, *J Wrist Surg* 13 (3) (2024) 194–201.
- [35] Y. Guo, et al., A comparison between robotic-assisted scaphoid screw fixation and a freehand technique for acute scaphoid fracture: a randomized, Controlled Trial, *J. Hand Surg. Am.* 47 (12) (2022) 1172–1179.
- [36] A.D. Heinzelmann, G. Archer, R.R. Bindra, Anthropometry of the human scaphoid, *J. Hand Surg. Am.* 32 (7) (2007) 1005–1008.
- [37] D.K. Smith, Anatomic features of the carpal scaphoid: validation of biometric measurements and symmetry with three-dimensional MR imaging, *Radiology* 187 (1) (1993) 187–191.
- [38] A. Arsalan-Werner, M. Sauerbier, I.M. Mehling, Current concepts for the treatment of acute scaphoid fractures, *Eur. J. Trauma Emerg. Surg.* 42 (1) (2016) 3–10.
- [39] M. Haefeli, et al., Titanium template for scaphoid reconstruction, *J Hand Surg Eur* 40 (5) (2015) 526–533.
- [40] P. Honigmann, et al., In-hospital 3D printed scaphoid prosthesis using medical-grade polyetheretherketone (PEEK) biomaterial, *Biomed. Res. Int.* 2021 (2021) 1301028.
- [41] A. Schweizer, et al., Computer-assisted 3-dimensional reconstructions of scaphoid fractures and nonunions with and without the use of patient-specific guides: early clinical outcomes and postoperative assessments of reconstruction accuracy, *J. Hand Surg. Am.* 41 (1) (2016) 59–69.
- [42] H.W. Yin, et al., 3D printing-assisted percutaneous fixation makes the surgery for scaphoid nonunion more accurate and less invasive, *J. Orthop. Translat.* 24 (2020) 138–143.
- [43] J.K. Kim, J.O. Yoon, H. Baek, Corticocancellous bone graft vs cancellous bone graft for the management of unstable scaphoid nonunion, *Orthop. Traumatol. Surg. Res.* 104 (1) (2018) 115–120.
- [44] K.K. Amrami, M.A. Frick, J.M. Matsumoto, Imaging for acute and chronic scaphoid fractures, *Hand Clin.* 35 (3) (2019) 241–257.